Fluctuations of Electrical Conductivity: A New Source for Astrophysical Magnetic Fields

F. Pétrélis, A. Alexakis, and C. Gissinger

Laboratoire de Physique Statistique, Ecole Normale Supérieure, CNRS, Université Pierre et Marie Curie,
Université Paris Diderot, 24 rue Lhomond, 75005 Paris, France

We consider the generation of a magnetic field by the flow of a fluid for which the electrical conductivity is nonuniform. A new amplification mechanism is found which leads to dynamo action for flows much simpler than those considered so far. In particular, the fluctuations of the electrical conductivity provide a way to bypass antidynamo theorems. For astrophysical objects, we show through three-dimensional global numerical simulations that the temperature-driven fluctuations of the electrical conductivity can amplify an otherwise decaying large scale equatorial dipolar field. This effect could play a role for the generation of the unusually tilted magnetic field of the iced giants Neptune and Uranus.

The current explanation for the existence of a magnetic field in astrophysical objects was given in 1919 by Larmor [1]. The motion of an electrically conducting fluid amplifies a seed of magnetic field by induction: this is the dynamo instability. Despite nearly a hundred years of research, several questions remain open. One of the reasons is that, for a flow to be dynamo active, it has to be complex enough.

For instance, for a fluid with uniform physical properties, planar flows cannot create magnetic fields [2]. This result, together with other similar antidynamo theorems [3], severely constrains the structure of the flows that can act as dynamos. Broadly speaking, both the flow and the resulting magnetic field must be complex enough.

In an astrophysical object, considering the electrical conductivity σ as a constant is a very crude simplification. In most natural situations (liquid core of planetary dynamos, plasmas of stellar convection zones, galaxies), the temperature T, the chemical compositions C_i, and the density of the fluid ρ are expected to display large variations. As a result, the electrical conductivity of the fluid is unlikely to remain uniform in the bulk of the flow. In other words, σ, that is determined by ρ, T, and C_i can be written as a function of space and time $\sigma(r, t)$ because ρ, T, and C_i are functions of space and time. The effect of a boundary of varying conductivity close to a flow tangent to the boundary had been considered to model inhomogeneities of the Earth mantle [4]. A dynamo instability has been predicted but requires a flow with a huge velocity [5]. In this article, we describe how magnetic field generation is affected by conductivity variations in the bulk of the fluid.

To calculate this effect, we have to take into account that σ depends on position in the equation for the magnetic field that reads

$$\frac{\partial \mathbf{B}}{\partial t} = \nabla \times (\mathbf{v} \times \mathbf{B}) - \nabla \times \left[\frac{1}{\sigma} \nabla \times \left(\frac{\mathbf{B}}{\mu_0} \right) \right]. \quad (1)$$

Insight can be obtained using the approximation of scale separation. We assume that the velocity and conductivity fields are periodic of period l. We note $\langle \cdot \rangle$ the spatial average over l. Let the magnetic diffusivity be $\eta = (\mu_0 \sigma)^{-1} = \eta_0 + \delta\eta$, where η_0 is the mean of η and $\delta\eta$ its variations. We write $\mathbf{B} = \langle \mathbf{B} \rangle + \mathbf{b}$ and consider that $\langle \mathbf{B} \rangle$ varies on a very large scale compared to l. In this limit, $\langle \mathbf{B} \rangle$ satisfies a mean-field (closed) equation that reads

$$\frac{\partial \langle \mathbf{B} \rangle}{\partial t} = \nabla \times (\alpha \langle \mathbf{B} \rangle) + \eta_0 \nabla^2 \langle \mathbf{B} \rangle, \quad (2)$$

where $\alpha \langle \mathbf{B} \rangle$ is the sum of two terms,

$$\alpha \langle \mathbf{B} \rangle = \langle \mathbf{v} \times \mathbf{b} \rangle - \langle \delta\eta \nabla \times \mathbf{b} \rangle. \quad (3)$$

Provided that $\delta\eta$ and the small scale field are small compared to, respectively, η_0 and the large scale field, $\mathbf{b}$ is solution of

$$\frac{\partial \mathbf{b}}{\partial t} - \eta_0 \nabla^2 \mathbf{b} = \langle \mathbf{B} \rangle \cdot \nabla \mathbf{v}, \quad (4)$$

such that by virtue of scale separation $\mathbf{b}$ can be calculated as a function of the large scale field $\langle \mathbf{B} \rangle$. Then α is obtained which closes Eq. (2). The term $\langle \mathbf{v} \times \mathbf{b} \rangle$ is the usual alpha effect [3] and writes $\langle \mathbf{v} \times \mathbf{b} \rangle = \alpha^h \langle \mathbf{B} \rangle$. The tensor α^h can be expressed using the Fourier transform of the velocity field $\hat{\mathbf{v}} = (2\pi)^{-3/2} \int \mathbf{v} \exp(i\mathbf{k}r) d^3 r$, where for simplicity we have set $l = 2\pi$ in all directions. We obtain

$$\alpha^h_{u,j} = (2\pi)^{-3} i \Sigma_k \frac{\mathbf{k}_j}{\eta_0 \mathbf{k}^2} [\hat{\mathbf{v}}(-\mathbf{k}) \times \hat{\mathbf{v}}(\mathbf{k})]_u. \quad (5)$$

This is the usual result for the α tensor in a homogeneous fluid. The second term in Eq. (3) is new and reads

$$\alpha_{u,j}^{\sigma}\langle \mathbf{B}_j \rangle = -\langle \delta\eta \nabla \times \mathbf{b} \rangle$$

$$= (2\pi)^{-3}\Sigma_k \frac{\mathbf{k}\cdot\langle \mathbf{B} \rangle}{\eta_0 \mathbf{k}^2}\hat{\delta\eta}(-\mathbf{k})[\mathbf{k}\times\hat{\mathbf{v}}(\mathbf{k})]_u. \quad (6)$$

Introducing the vorticity $\Omega = \nabla \times \mathbf{v}$, the new part of the α tensor can be written

$$\alpha_{u,j}^{\sigma} = -(2\pi)^{-3}i\Sigma_k \frac{\mathbf{k}_j}{\eta_0 \mathbf{k}^2}[\hat{\delta\eta}(-\mathbf{k})\hat{\Omega}_u(\mathbf{k})]$$

$$= (2\pi)^{-3}\Sigma_k \frac{\widehat{\partial_j \delta\eta}(-\mathbf{k})\hat{\Omega}_u(\mathbf{k})}{\eta_0 \mathbf{k}^2}$$

$$= -(2\pi)^{-3}\Sigma_k \frac{\hat{\delta\eta}(-\mathbf{k})\widehat{\partial_j \Omega}_u(\mathbf{k})}{\eta_0 \mathbf{k}^2}. \quad (7)$$

Large values of α^{σ} thus require strong correlations between diffusivity variations and gradients of the vorticity or, equivalently, between gradients of diffusivity and vorticity. This can be understood by considering a vortical flow in which the vorticity is modulated in the ϕ direction, a classical picture of convective flows in planetary cores, as sketched in Fig. 1. Assume that a large scale magnetic field is applied in the ϕ direction. Calculating $\mathbf{v} \times \mathbf{B}$, we observe that currents of opposite signs are induced in the vertical z direction. Then, the azimuthal variation of electrical conductivity strengthens the current in one direction and reduces it in the opposite one. This results in a total electric current flowing in the z direction as predicted by our calculation. This current can in turn amplify the magnetic field.

Having identified the pertinent properties of the velocity and conductivity fields, we now discuss one example. Let the velocity be $\mathbf{v} = (A\cos(ky)\sin(kz),$ $B\cos(kx)\sin(kz), 0)$ and the diffusivity variation be $\delta\eta/\eta_0 = \delta(\cos(kz)(\sin(ky) - \sin(kx)))$. The velocity field is a periodic array of counterrotating vortices located in the x-y planes. The amplitude of the velocity field is simply modulated in the z direction. The α tensor reads $\langle \mathbf{v} \times \mathbf{b} \rangle = 0$ and $\langle -\delta\eta\nabla \times \mathbf{b} \rangle = \delta/8(BBx, ABy, -(A+B)Bz)$. We then calculate the growth rate p for a large scale mode proportional to $\exp(pt + iKz)$ and obtain $p = (|\delta K|\sqrt{AB}/8) - \eta_0 K^2$. Dynamo instability is possible provided $\mathrm{Rm} = |\delta|\sqrt{AB}/(\eta_0|K|) > 8$. We point out that for this flow, in the absence of conductivity variation, no dynamo would be possible.

The asymptotic results derived here were confirmed using numerical simulations. To achieve large scale separation, we used a code based on Floquet theory, allowing us to write the solutions of Eq. (1) as $\mathbf{B}(\mathbf{x}, t) = e^{i\mathbf{K}\cdot\mathbf{x}}\mathbf{b}(\mathbf{x}, t)$, where $\mathbf{K}$ is an arbitrary wave number and $\mathbf{b}(\mathbf{x}, t)$ is a space-periodic vector field with the same period as $\mathbf{v}$ and η. The numerically calculated growth rates for the flow are shown in Fig. 2 for $\mathrm{Rm} = 1/6$ and different values of $\mathbf{K}$ and $\delta\eta$, and show an excellent agreement with the asymptotic results. Note that, because of scale separation, even small values of the diffusivity variation $\delta\eta$ lead to a dynamo.
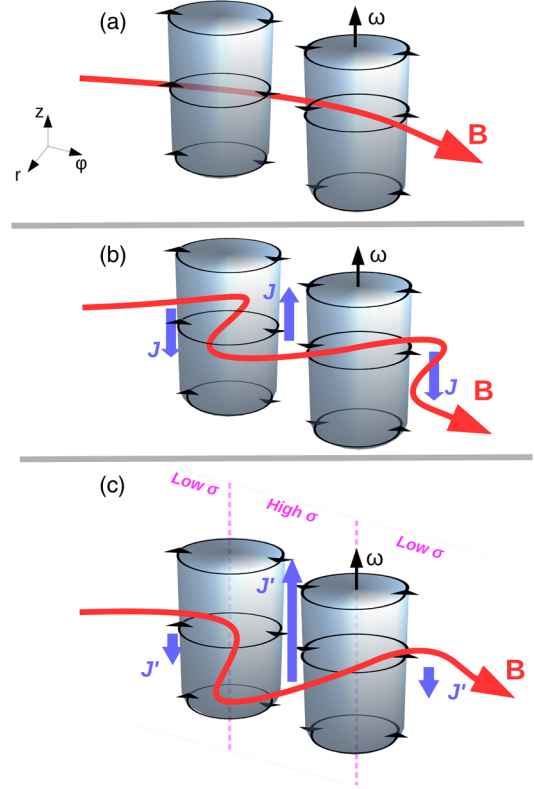

FIG. 1. Sketch of the different steps involved in the amplification mechanism α^{σ} for a typical geophysical flow. Top: Two adjacent convective cells (gray cylinders) with axial vorticity ω are subject to a transverse azimuthal magnetic field B (red). Middle: Both upward and downward axial currents $J \propto (\mathbf{v} \times \mathbf{B})$ (blue) are induced between the convective cells. Bottom: In the presence of conductivity gradients correlated to the vorticity (maximum gradient represented by pink dashed lines), large (respectively, low) conductivity increases (respectively, decreases) the induced current: the resulting net upward current J' is parallel to the vorticity.
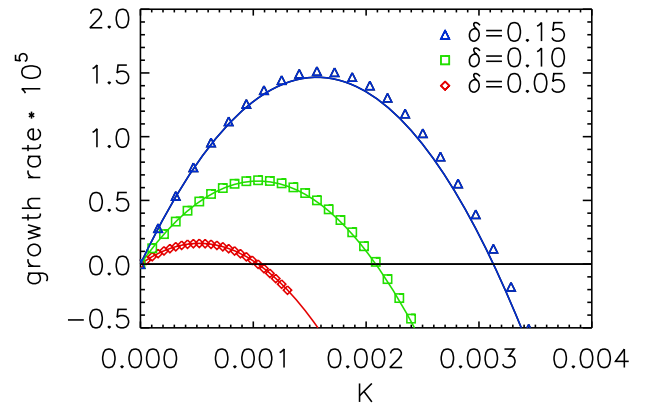

FIG. 2. The growth rates for the 2D flow considered in the text as a function of $\mathbf{K}$, for $\mathrm{Rm} = 1/6$ and three different $\delta\eta$. Symbols correspond to numerically evaluated growth rates and straight lines to the analytical prediction.

This mechanism provides a simple way to bypass antidynamo theorems and may thus play a role in the creation of magnetic fields of astrophysical objects. As a first step towards answering this question, we have considered the generation of magnetic field by the flow of a thermally convecting Boussinesq fluid contained in a rotating spherical shell, thus modeling stellar or planetary core configurations. Fixed temperatures are imposed at both inner and outer boundaries, no-slip boundary conditions are used for the velocity field, and both boundaries are electrically insulating. The dimensionless parameters are the shell aspect ratio $\gamma = r_i/r_o$, the magnetic Prandtl number $\mathrm{Pm} = \nu/\eta_0$, the Ekman number $E = \nu/\Omega D^2$, and the Rayleigh number $\mathrm{Ra} = \alpha g_0 \Delta T D/(\nu\Omega)$, where $D = r_o - r_i$ is the gap and Ω, ν, η_0, κ, α, and g_0 are, respectively, the rotation rate, the kinematic viscosity, the spatially averaged magnetic diffusivity, the thermal diffusivity, the thermal expansion coefficient, and the gravity at the outer sphere. Equations of magnetohydrodynamics for the velocity v, magnetic field B, and temperature T are solved with the help of the code PaRoDy [6], which has been modified to take into account the spatial variation of the electrical conductivity. As a simple example, we assume here that the magnetic diffusivity η depends on the temperature as $\eta = \eta_0 + k(T - T_0)$, where the proportionality coefficient k is kept as a control parameter. Several configurations have been considered: conductivity depending only on the temperature fluctuations or on both the temperature fluctuations and the background temperature profile. In addition, different widths of the spherical shell have been tested. Note that effects of radially varying conductivity were studied in [7], in which it was shown that a low-conductivity layer close to the core-mantle boundary may explain Mercury's weak observable magnetic field. Here, we rather study the case of conductivity depending on the temperature field that can fluctuate in all directions.

Although the parameter space is huge and further work is required to fully characterize the effect of a varying conductivity, it can be identified that a transverse dipolar field benefits from a modulation of electrical conductivity in typical geodynamo simulations. Figure 3 shows the growth rate of the magnetic field as a function of the amplitude of the conductivity modulation for $\gamma = 0.35$, $E = 6 \times 10^{-4}$, $\mathrm{Ra}/\mathrm{Ra}_c = 2.2$ (Ra = 123), and Pm = 7.9. In the case of an homogeneous conductivity ($\delta\eta/\eta_0 = 0$), an axial dipole is observed (black curve), as usual for these parameters. As the coupling coefficient k between the temperature and the conductivity is increased, the growth rate of this dipole decreases until it becomes kinematically stable. In contrast, the growth rate of the equatorial dipole mode (red curve) increases from negative to positive values. As soon as $\delta\eta/\eta_0$ reaches 5%, the modulation of the electrical conductivity changes the structure of the dynamo field, replacing the axial dipole by a transverse one. For both modes, we observe a linear relation between the growth rate and the conductivity modulation, as predicted by our theory.

This effect of the conductivity modulation is observed in a wide region of the parameter space. For instance, Fig. 4 displays the spatial structure of the dynamo magnetic field obtained for $E = 10^{-3}$, $\mathrm{Ra}/\mathrm{Ra}_c = 2$, Pm = 7, and $\delta\eta/\eta_0 = 0.4$, corresponding to an equatorial dipolar field. Note that for these values of E and Ra, the conductivity fluctuations decrease the dynamo onset by roughly 20% compared to the homogeneous case.
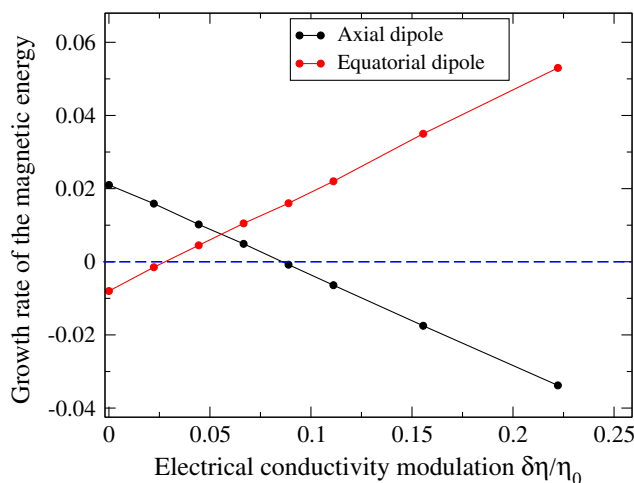

FIG. 3. Growth rate of the magnetic energy in the kinematic phase as a function of the (temperature-driven) electrical conductivity modulation in a dynamo simulation, for $E = 6 \times 10^{-4}$, Pm = 7.9, and $\mathrm{Ra}/\mathrm{Ra}_c = 2.2$, for axial (black) and equatorial (red) dipole modes. Note that the axial dipole obtained at $\delta\eta/\eta_0 = 0$ is replaced by a transverse dipole in presence of conductivity modulation.
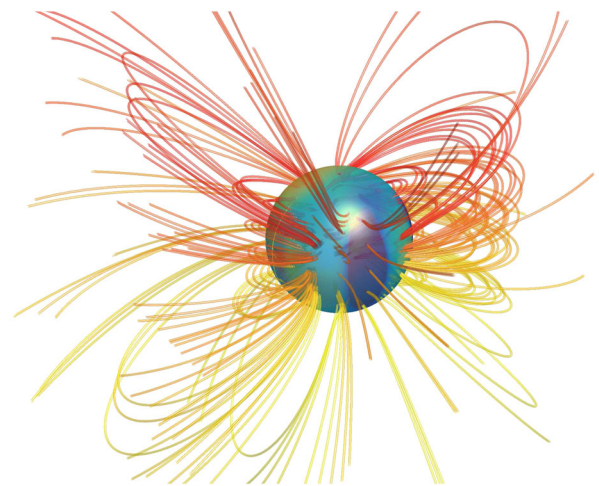

FIG. 4. Structure of the saturated equatorial dipole generated for $E = 10^{-3}$, Pm = 7, $\mathrm{Ra}/\mathrm{Ra}_c = 2$, and $\delta\eta/\eta_0 = 0.4$. The colored sphere indicates amplitude of the radial magnetic field at the surface of the core-mantle boundary and magnetic field lines in the insulating mantle are shown.
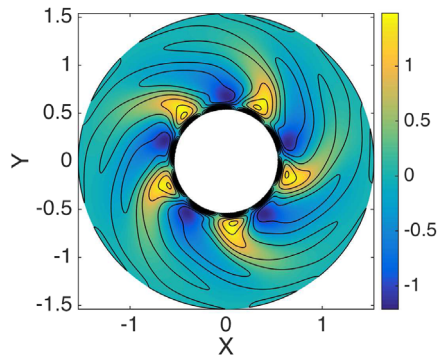
FIG. 5. Equatorial cut of the purely hydrodynamical state obtained for $E = 6 \times 10^{-4}$ and $\mathrm{Ra}/\mathrm{Ra}_c = 2.2$. The color plot displays the amplitude of the azimuthal temperature gradient $\partial_\phi T$, whereas black lines are isocontours of the axial component of the vorticity $(\nabla \times \mathbf{u}) \cdot \mathbf{e_z}$. Note the strong correlation between the two quantities.

To understand how such a temperature-dependent conductivity decreases the dynamo onset, it is important to note that geophysical flows, strongly affected by Taylor-Proudman theorem, mainly consist of several columnar vortices arranged along the azimuthal direction (the so-called Busse columns [8]) with temperature gradient maximum at the center of the vortices. This convective pattern is therefore characterized by a strong correlation between the axial vorticity and the azimuthal gradient of temperature, as illustrated in Fig. 5. The component $(\nabla \times \mathbf{u})|_z \cdot \nabla_\phi(\delta\eta)$ is mainly localized in the equatorial plane, thus suggesting that this nondiagonal term of the α^σ tensor is responsible for the generation of the field. Note that this differs from the diagonal part of the usual α effect, which vanishes in the equatorial plane. The α^σ effect, being strong in the equatorial plane, thus provides a possible explanation for the equatorial dipolar component of the magnetic field observed in Neptune and Uranus [9,10].

To discuss further the relevance of this effect, it is interesting to compare its efficiency with the one of an α^2 dynamo. In scale separation, the onset for an α^2 dynamo is given by $V\sqrt{lL}/\eta = C_1$, where C_1 is a constant, V is the amplitude of the velocity, l is the wavelength of the flow, and L is the size over which the large scale field varies. For an α^σ dynamo, the onset is $\delta V L/\eta = C_2$, where C_2 is a constant and δ the amplitude of the relative variations of conductivity. Thus, for a flow that is prone to both effects, the α^σ dynamo leads to a smaller onset provided $\delta\sqrt{L/l} \gg 1$, meaning that this new kind of dynamo is expected when scale separation is large enough.

As the efficiency of the α^σ effect depends crucially on the variations of the electrical conductivity, it is worth discussing possible sources for these variations that are met in nature. In a telluric planet such as the Earth, the time-averaged electrical conductivity varies with the depth in the liquid core due to the increase of temperature and pressure [11]. However, one has to consider the effect of the

convective temperature fluctuations which are quite smaller than the static radial variations. These fluctuations are the sources of both the conductivity variations and the velocity fluctuations, and simple estimates of their intensities show that the efficiency of the α^σ effect is larger than the one of the usual α effect when scale separation is large enough. It is then worth noting that rapid rotation results in a drastic shortening of the characteristic length scale of convective pattern [12], so that this new kind of dynamo should be relevant for rapidly rotating astrophysical objects.

In the case of the Sun, temperature differences of 200–400 K are measured at the surface between ascending and descending plumes. For linear dependance of σ on T, this would correspond to relative variations of σ of 3% to 7%, making the dimensionless parameter $\delta V L/\eta$ large enough for the α^σ effect to play a role.

The magnetic field is known to play a role in the dynamics of the Sun convective zone. This sheds light on another possible source for conductivity variations: Ohmic dissipation itself. On can imagine that the electric currents heat up locally the fluid so that it modifies the conductivity and affects the efficiency of the α^σ effect. This would result in a nonlinear mechanism that could act as a saturation mechanism if the efficiency of the effect is decreased by Joule heating or, if the efficiency is increased, could be responsible for a nonlinear amplification. This effect thus provides a new scenario for a subcritical dynamo instability.

In the laboratory, the α^σ effect can be used to build dynamo flows simpler than those considered so far. Indeed, the possibility to use planar flow greatly simplifies the geometrical constraints. Using liquid sodium which displays a decrease of conductivity of more than 25% between 100 and 200 degrees, a periodic array of counterrotating vortices with proper control of temperature variations would generate a dynamo at a magnetic Reynolds number achievable at the laboratory scale.

Finally, one may use the α^σ effect to modify the onset of an existing laboratory dynamo setup. The Karlsruhe dynamo [13] is the simplest configuration to analyze, as it is made of a periodic array of helical flows. By imposing conductivity variations between the different vortices, an α^σ effect is added to the α effect. A corresponding decrease of the critical magnetic Reynolds number proportional to $\delta\eta/(Vl)$ is expected, leading to a possible threshold reduction of roughly 10%.

[1] J. Larmor, Br. Assoc. Adv. Sci. Rep. **87**, 159 (1919).

[2] Y. Zeldovich and A. Ruzmaikin, Sov. Phys. JETP **51**, 493 (1980).

[3] H. K. Moffatt, *Magnetic Field Generation in Electrically Conducting Fluids* (Cambridge University Press, Cambridge, 1978).

[4] F. Busse and J. Wicht, Geophys. Astrophys. Fluid Dyn. **64**, 135 (1992).

[5] This is discussed in detail in the similar situation of a varying magnetic permeability by B. Gallet, F. Pétrélis, and S. Fauve, Europhys. Lett. **97**, 69001 (2012); B. Gallet, F. Pétrélis, and S. Fauve, J. Fluid Mech. **727**, 161 (2013).

[6] E. Dormy, P. Cardin, and D. Jault, Earth Planet. Sci. Lett. **160**, 15 (1998).

[7] N. Gomez-Perez, M. Heimpel, and J. Wicht, Phys. Earth Planet. Inter. **181**, 42 (2010).

[8] F. H. Busse, J. Fluid Mech. **44**, 441 (1970).

[9] N. F. Ness, M. H. Acuna, K. W. Behannon, L. F. Burlaga, J. E. P. Connerney, R. P. Lepping, and F. M. Neubauer, Science **233**, 85 (1986); N. F. Ness, M. H. Acuna, L. F. Burlaga, J. E. P. Connerney, R. P. Lepping, and F. M. Neubauer, Science **246**, 1473 (1989).

[10] For other possible explanations of the equatorial component of the iced giant magnetic field, see S. Stanley and J. Bloxham, Nature (London) **428**, 151 (2004); J. Aubert and J. Wicht, Earth Planet. Sci. Lett. **221**, 409 (2004); C. Gissinger, L. Petitdemange, M. Schrinner, and E. Dormy, Phys. Rev. Lett. **108**, 234501 (2012).

[11] H. Gomi, K. Ohta, K. Hirose, S. Labrosse, R. Caracas, M. J. Verstraete, and J. W. Hernlund, Phys. Earth Planet. Inter. **224**, 88 (2013).

[12] S. Chandrasekhar, *Hydrodynamic and Hydromagnetic Stability* (Clarendon Press, Oxford, 1961).

[13] R. Stieglitz and U. Müller, Phys. Fluids **13**, 561 (2001).